RADAR AND IN SITU OBSERVATIONS IN A WINTER BOW ECHO AND ASSOCIATED MESO-VORTICES OVER THE JAPAN SEA AREA

Kenichi Kusunoki[1], Hanako Inoue[1], Masahisa Nakazato[1], Kotaro Bessho[1], Shunsuke Hoshino[1], Wataru Mashiko[1], Syugo Hayashi[1], Hiroyuki Morishima[2], Keiji Adachi[2]

[1] *Meteorological Research Institute, 1-1, Nagamine, Tsukuba 305-0052, Japan, kkusunok@mri-jma.go.jp,*
[2] *East Japan Railway Company, 2-479, Nisshin-cho, Kita-ku, Saitama 331-8513, Japan, h-morishima@jreast.co.jp*

(Dated: 26 August 2011)

I. INTRODUCTION

On Japan railroads, wind conditions affect operating efficiency, infrastructure, and safe passage of people and freight. For instance, strong and gusty winds cause regional delays or shutdowns, and especially hazardous crosswinds may lead to overturn of railcars. Since propeller-vane/cup anemometers densely cover on the railroads for operations through some wind speed thresholds (e.g., winds in excess of 25 ms^{-1}), small-scale but strong gusty winds are difficult to detect with the present system. The Shonai area railroad weather project will investigate fine-scale structure of wind gust dynamics and kinetics such as tornadoes, downbursts, and gust fronts. The ultimate goal of the project is to develop an automatic strong gust detection system for railroads, which the decision to warn is generally based upon information from a single-Doppler radar at low elevation angles. In this presentation, we will introduce radar and in-situ measurement in a winter bow echo on January 24 2008.

II. INSTRUMENTATION

Figure 1 shows the study area where the high-resolution observations of strong gust phenomena have been performed over the Shonai area (Yamagata Pref., Japan). Primarily, over the Sea of Japan side, severe storms such as tornadoes and gust-generating cold fronts occur frequency in winter season. The study area would provide an ideal setting for studying these phenomena (Kusunoki et al. 2007). Major observing instrumentation for this project included the two X-band Doppler radars and the network of automated weather station sites.

Especially, the JR EAST X-band Doppler radar provided the data used in this presentation. The JR EAST X-band Doppler radar was installed at the Amarume station in Shonai Town since March 2007. Since it is needed to observe wind gusts successfully, the radar is operated in a single PPI mode at the lowest elevation angle possible to provide the reflectivity and Doppler velocities as close to the ground. The single elevation angle is 3.0 degree and the scans are taken every 30sec (Kato et al. 2007).

III. RESULTS

A bow echo associated with a winter convective line traversed across the Shonai area on 24 January 2008. Figure 2 indicates the bow echo observed with the JR-E Doppler radar. The orientation was south to north and moved to the northeast at about 25ms^{-1}. At 03:18:04 LST, the radar pattern indicates that the maximum length of the bow echo was about 18km, with a sharp reflectivity gradient and enhanced low-level convergence ahead. It is clearly indicated that an intense wind core was located at the bow apex. During the declining stage (03:26:19 LST), the figure reveals clearly the transition from the bow shaped echo to comma-shaped echo. This evolution is similar to those seen in previous studies (Fujita 1978). Note that the rear inflow notch is difficult to identify clearly in this case because of the beam blockage of the low elevation angle (3.0degree).

Figure 3 shows the bow echo positions during its landfall. Shading in this figure represents an intense Doppler velocity core exceeding 25 ms^{-1}. The location of the intense wind core is consistent with the location of rear-inflow jets (RIJs) at the apex of bow echoes that previous radar studies have documented (e.g., Przybylinski 1995; Funk et al. 1999; Atkins et al. 2004). The region of the bow apex was passed over the Shonai Airport at around 0321 LST, which is located about 1.5 km from the shoreline. In situ surface data at the Shonai Airport for the bow apex are shown in Figure 4. Associated with the intense wind core, the wind data confirmed a maximum wind 22.6 ms^{-1} but little wind direction shift. This wind gust

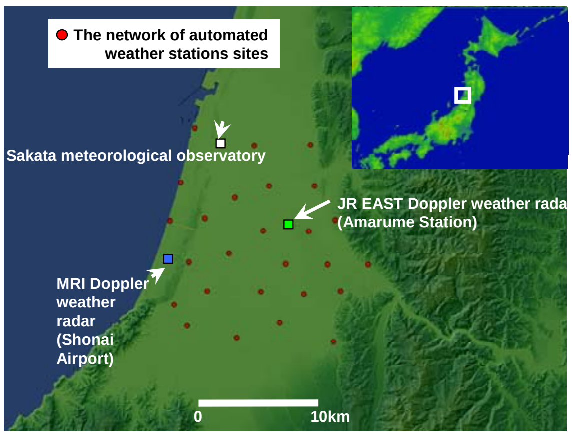

FIG. 1 Map of the Shonai area. Closed circles are the network of automated weather station sites. The inset shows the locations of the Sea of Japan and the study area (in the square).

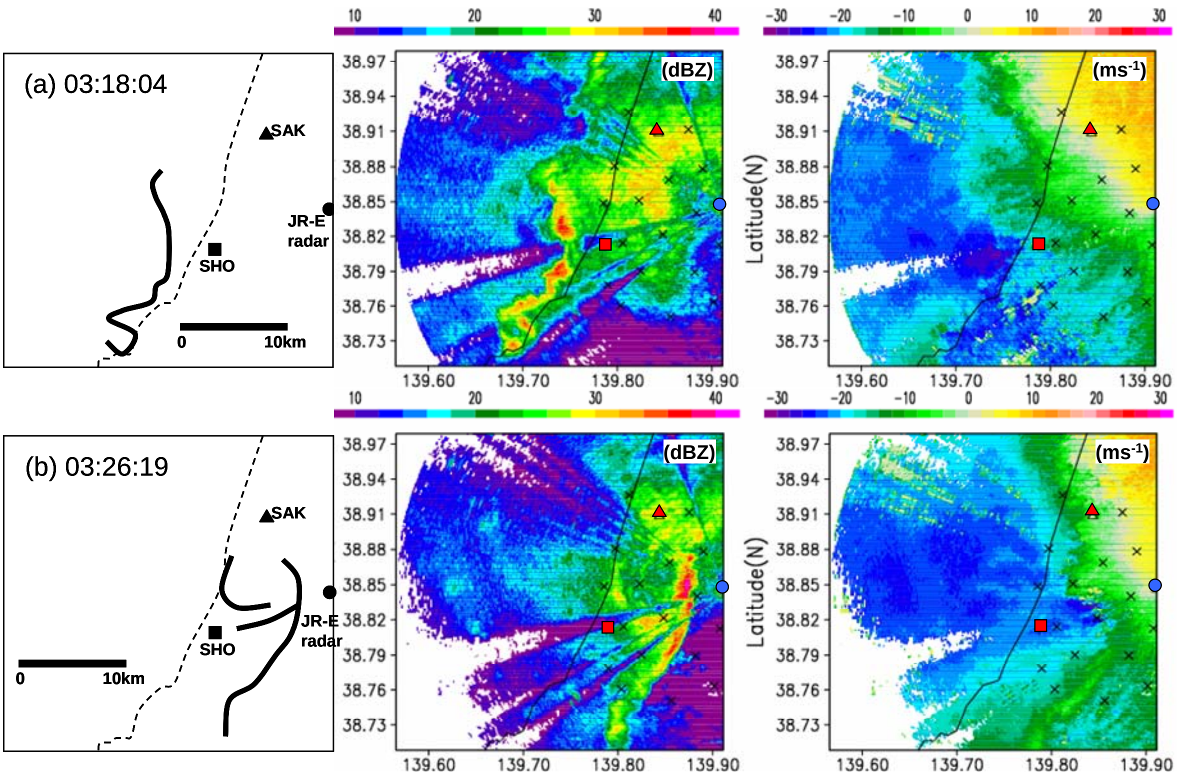

FIG. 2. Color PPI scans of reflectivity (center) and Doppler velocity (right) from the JR-E radar located at the Amarume station at elevation angle of 3.0 at (a) 03:18:04 and (b) 03:26:19 LST. The bow and comma echo locations are shown in the left panel. The bold lines represent reflectivities greater than approximately 30 dBZ. Filled square (SHO) is the Shonai Airport, filled triangle (SAK) is the Sakata meteorological observatory, and filled circle is the JR-E radar (Amarume Station). Cross marks (the center and right panels) are the network of automated weather station sites. Thin dashed line is the shoreline.

coincided with a rapid pressure rise and temperature and humidity drops, which closely resemble the kinematic character of gravity current. It is suggested that the intense straight-line wind may be created by a descending RIJ.

Another noticeable feature is several mesovortices observed along the leading edge of the bow (FIG. 3). In situ measurement data for a mesovortex embedded were obtained (FIG. 5). Surface wind gust that coincided with a surface pressure drop confirmed with the passage of a mesovortex over the Sakata meteorological observatory. In recent studies, Atkins and Laurent (2009) investigate the effect of bow echo mesovortices responsible for producing the strong surface wind. They concluded that the strongest surface winds were created the superposition of the RIJ and mesovortex flows. In this case, however, an interaction between the RIJ and mesovortices are not apparent in our analysis.

IV. ACKNOWLEDGMENTS

This study was supported by the Program for Promoting Fundamental Transport Technology Research from the Japan Railway Construction, Transport and Technology Agency (JRTT).

V. REFERENCES

Atkins, N. T., J. M. Arnott, R. W. Przybylinski, R. A. Wolf, and B. D. Ketcham, 2004: Vortex structure and evolution within bow echoes. Part I: Single-Doppler and damage analysis of the 29 June 1998 derecho. *Mon. Wea. Rev.*, **132**, 2224-2242.

Atkins, N. T., and M. St. Laurent, 2009: Bow echo mesovortices. Part I: Processes that influence their damaging potential. *Mon. Wea. Rev.*, **137**, 1497-1513.

Fujita, T. T., 1978: Manual of downburst identification for project Nimrod. Satellite and Mesometeorology Research Paper 156, Dept. of Geophysical Sciences, University of Chicago, 104 pp. [NTIS PB-286048.]

Funk, T. W., K. E. Darmofal, J. D. Kirkpatrick, V. L. DeWald, R. W. Przybylinski, G. K. Schmocker, and Y.-J. Lin, 1999: Storm reflectivity and mesocyclone evolution associated with the 15 April 1994 squall line over Kentucky and southern Indiana. *Wea. Forecasting*, **14**, 976-993.

Kato, W., H. Suzuki, M. Shimamura, K. Kusunoki, and T. Hayashi, 2007: The design and initial testing of an X-band Doppler radar for monitoring hazardous winds for railroad system. Preprints, *33rd Conf. on Radar Meteorology*, Cairns, Australia, Amer. Meteor. Soc. P13A.15.

Kusunoki, K., T. Imai, H. Suzuki, T. Takemi, K. Bessho, M. Nakazato, S. Hoshino, W. Mashiko, S. Hayashi, H. Inoue, T. Fukuhara, T. Shibata, W. Kato, 2008: An overview of the Shonai area railroad weather project and early outcomes Preprints, *Fifth Conference on Radar Meteorology and Hydrology*, Helsinki, 30 June - 4 July, 2008. P12.1.

Przybylinski, R. W., 1995: The bow echo: Observations, numerical simulations, and severe weather detection methods. *Wea. Forecasting*, **10**, 203-18.

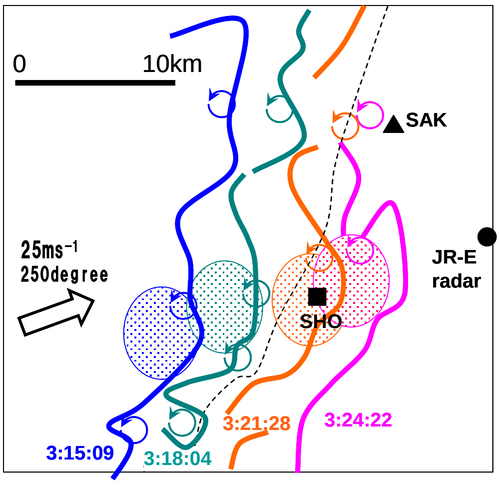

FIG. 3 The bow echo observed with the Doppler radar. Thick solid lines indicate bow echo locations at 3:15:09, 3:18:04, 3:21:28, and 3:24:22 LST 24 January 2008, respectively. Shading represents an intense Doppler velocity core exceeding 25 ms^{-1}. Thin circular arrows depict the positions of mesovortices. White arrow indicates the direction of the bow echoed motion. Symbols are same as FIG. 2.

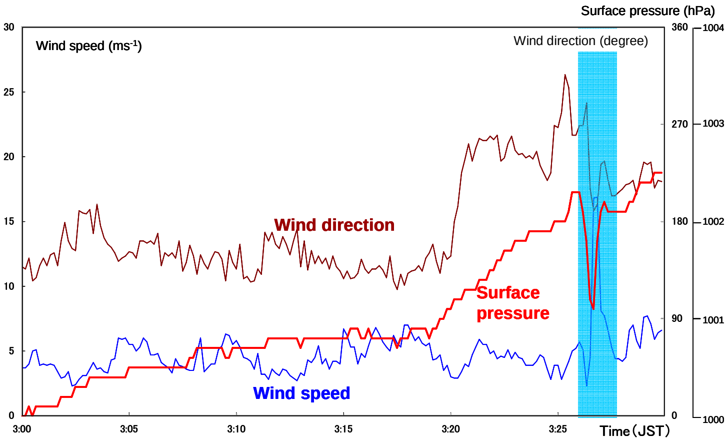

FIG. 5 Time series of surface wind speed, direction, and surface pressure from the Sakata meteorological observatory.

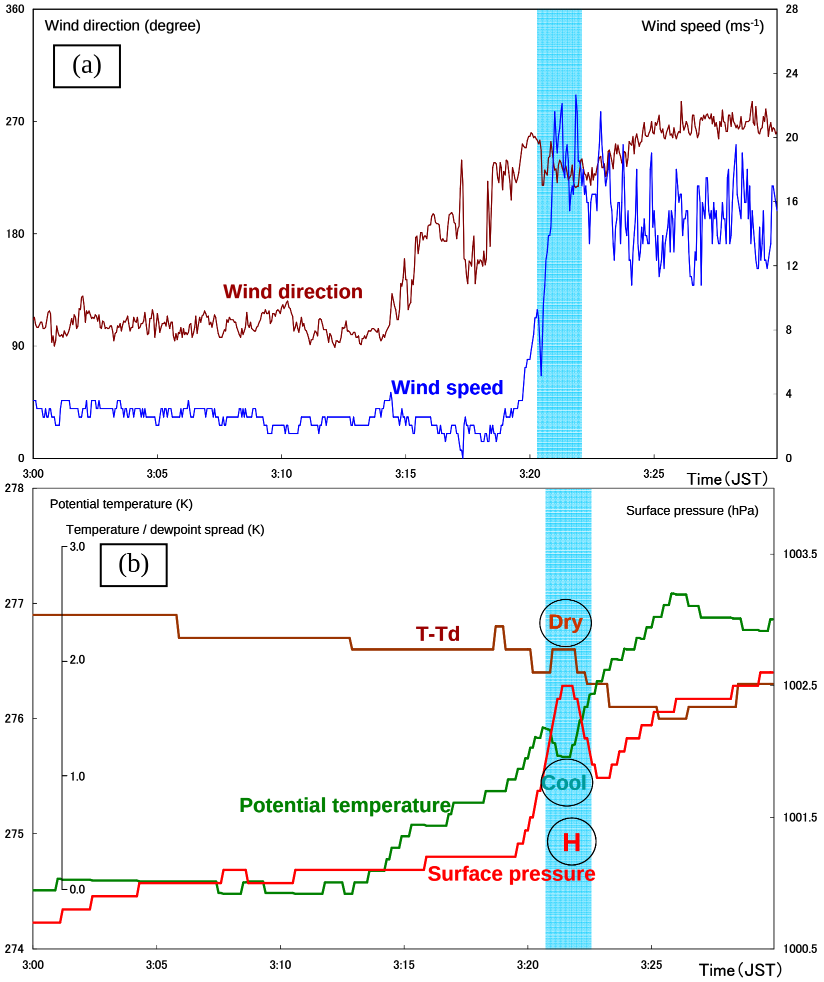

FIG. 4(a) Time series of surface wind speed and direction from the Shonai Airport. (b) Time series of surface pressure, temperature, and dewpoint depression (T-Td) from the Shonai Airport. The vertical hatchs indicate the wind gust period.